THE JOURNAL OF BIOLOGICAL CHEMISTRY VOL. 288, NO. 46, pp. 33292–33302, November 15, 2013

Identification of Wilms' Tumor 1-associating Protein Complex and Its Role in Alternative Splicing and the Cell Cycle*[S]

Received for publication, July 10, 2013, and in revised form, October 4, 2013 Published, JBC Papers in Press, October 7, 2013, DOI 10.1074/jbc.M113.500397

Keiko Horiuchi[‡], Takeshi Kawamura[‡], Hiroko Iwanari[‡], Riuko Ohashi[§], Makoto Naito[§], Tatsuhiko Kodama[¶], and Takao Hamakubo[‡1]

From the [‡]Department of Quantitative Biology and Medicine and the [¶]Laboratory for Systems Biology and Medicine, Research Center for Advanced Science and Technology, University of Tokyo, Tokyo 153-8904, Japan and the [§]Division of Cellular and Molecular Pathology, Niigata University Graduate School of Medical and Dental Sciences, Niigata 951-8510, Japan

Background: WTAP is a ubiquitously expressed nuclear protein that is required for mammalian early embryo development and cell cycle progression.
Results: WTAP forms a complex with several splicing regulators.
Conclusion: WTAP regulates both the cell cycle and alternative splicing by the formation of a protein complex.
Significance: Characterization of this protein complex will help to elucidate the critically important function of WTAP in alternative splicing and cell proliferation.

Wilms' tumor 1-associating protein (WTAP) is a putative splicing regulator that is thought to be required for cell cycle progression through the stabilization of cyclin A2 mRNA and mammalian early embryo development. To further understand how WTAP acts in the context of the cellular machinery, we identified its interacting proteins in human umbilical vein endothelial cells and HeLa cells using shotgun proteomics. Here we show that WTAP forms a novel protein complex including Hakai, Virilizer homolog, KIAA0853, RBM15, the arginine/serine-rich domain-containing proteins BCLAF1 and THRAP3, and certain general splicing regulators, most of which have reported roles in post-transcriptional regulation. The depletion of these respective components of the complex resulted in reduced cell proliferation along with G_2/M accumulation. Double knockdown of the serine/arginine-rich (SR)-like proteins BCLAF1 and THRAP3 by siRNA resulted in a decrease in the nuclear speckle localization of WTAP, whereas the nuclear speckles were intact. Furthermore, we found that the WTAP complex regulates alternative splicing of the *WTAP* pre-mRNA by promoting the production of a truncated isoform, leading to a change in WTAP protein expression. Collectively, these findings show that the WTAP complex is a novel component of the RNA processing machinery, implying an important role in both posttranscriptional control and cell cycle regulation.

Alternative splicing is the process by which multiple mRNAs are obtained from a single gene, thereby substantially increasing both protein diversity and complexity. Almost all of the transcripts of genes encoding multiple exons are alternatively spliced, and strict patterns of alternative splicing are critically important for health and normal development (1–3). The concept of alternative splicing as a major controller of gene expression was largely established on the basis of genetic studies of the *Drosophila* sex determination pathway, where female-specific expression of the RNA-binding protein SXL (sex-lethal) regulates the alternative splicing of *Sxl*, transformer, and *msl-2* (male-specific-lethal 2) pre-mRNA, which control sex-specific alternative splicing and/or translation of the genes responsible for sexual differentiation and behavior (4–8). Genetic analyses have revealed that three additional genes are required for female-specific alternative splicing of *Sxl*: *snf* (sans fille) (9), *vir* (virilizer) (10), and *fl(2)d* (11). Previous studies with FL(2)D (female lethal d) antibodies showed the physical interaction of FL(2)D with SXL (12, 13), VIR (12), Snf, U2AF, U2A50, and U2AF38 (13) in embryo nuclear extracts, suggesting that FL(2)D may act at an early step in the SXL-dependent regulation of alternative splicing.

Wilms' tumor 1-associating protein (WTAP),[2] a mammalian homologue of *fl(2)d*, was identified as a protein that specifically interacts with Wilms' tumor 1 (WT1) in both *in vitro* and *in vivo* assays (14). WTAP and WT1 are present together throughout the nucleoplasm as well as in speckles and colocalize in part with splicing factors (14). In addition, WTAP has been found in functional human spliceosomes (15). Other proteomic studies have also isolated WTAP as a component of the interchromatin granule clusters that correspond to nuclear speckles, where a variety of proteins involved in gene expression, such as transcription factors and splicing factors, are assembled, modified and sorted (16). Thus, WTAP is considered to have an evolutionarily conserved role in the regulation of splicing in mammalian cells. However, the detailed molecular mechanism is not well understood, although its essential role has been established in mouse early embryo development and cell cycle regulation (17, 18).

We previously reported that WTAP is required for G_2/M cell cycle transition through the stabilization of cyclin A2 mRNA

* This work was supported by Grants-in-aid for Scientific Research 20221010 and 08104737 from the Ministry of Education, Culture, Sports, Science, and Technology of Japan.
[S] This article contains supplemental Tables S1 and S2.
[1] To whom correspondence should be addressed. Tel./Fax: 81-3-5452-5231; E-mail: hamakubo@qbm.rcast.u-tokyo.ac.jp.

[2] The abbreviations used are: WTAP, Wilms' tumor 1-associating protein; aa, amino acids; RIP, RNA co-immunoprecipitation; HUVEC, human umbilical vein endothelial cell.

and is vital for early mouse development (17). WTAP stabilizes cyclin A2 mRNA through the 3′-UTR sequence, and a suppression of WTAP expression by siRNA resulted in G_2 phase accumulation in HUVECs and human neonatal dermal fibroblasts. On the other hand, Small *et al.* (19, 20) reported that WTAP inhibits SMC proliferation and activates apoptosis by modulating the alternative splicing of the apoptosis regulator survivin. In addition, recent studies have shown that WTAP is overexpressed in glioblastoma (21) and cholangiocarcinoma (22) and promotes the migration and invasion of these cancer cells with an effect on cell proliferation under a condition of 1% FBS. The cell type-specific effect of WTAP on cell proliferation suggests a sensitive dependence on the cellular context, such as the requisite presence of certain binding partners.

In the work presented here, we generated anti-WTAP monoclonal antibodies and identified the proteins that interact with WTAP using shotgun proteomics. The components of the WTAP complex are enriched in proteins that are involved in post-transcriptional regulation, such as pre-mRNA splicing, mRNA stabilization, polyadenylation, and/or mRNA export. Among them, double knockdown of the SR-like proteins BCLAF1 (BCL2-associated transcription factor 1) and THRAP3 (thyroid hormone receptor-associated protein 3) resulted in a decrease in the speckle localization of WTAP, whereas the nuclear speckles were intact. Depletion of the major components of the complex, such as Virilizer homolog, KIAA0853, BCLAF1/THRAP3, Hakai, and RBM15 (RNA-binding motif protein 15) resulted in reduced cell proliferation with G_2 phase accumulation. Moreover, we found that the WTAP complex regulates alternative splicing of the *WTAP* pre-mRNA and, thereby, the expression of full-length WTAP protein. Taken together, our findings suggest that WTAP localizes to nuclear speckles through the interaction of BCLAF1 or THRAP3 and thus takes part in posttranscriptional regulation.

EXPERIMENTAL PROCEDURES

Cell Culture—HUVECs (Lonza) were cultured in EGM2 medium (culture medium supplemented with growth factors) (Lonza) and used within the first six passages. HeLa and HEK293T cells were grown in Dulbecco's modified Eagle's medium supplemented with 10% fetal bovine serum.

Antibodies—The expressed GST-full-length human WTAP protein (396 amino acids (aa)) was purified on glutathione-agarose beads (Sigma) and injected into BALB/c mice to produce the monoclonal antibodies H1122 and H1137. The Y6828 monoclonal antibody against the human WTAP N terminus was raised using a baculoviral display system, as described previously (23). Monoclonal antibodies for Virilizer (Y1639, aa 1421–1480 were used as the immunogen), Hakai (Y6048, aa 430–491), and RBM15 (Z9701, aa 430–491) were also generated. Polyclonal anti-human WTAP antibodies raised in rabbits were used for immunoblotting (17). The following antibodies were purchased and used: BCLAF1 (A300-608A, Bethyl), THRAP3 (A300-956A, Bethyl), Virilizer (A302-124A, Bethyl), KIAA0853 (ab70802, Abcam), Hakai (ARP39623_T100, Aviva Systems Biology), RBM15 (ab70549, Abcam), V5 (R960-25, Invitrogen), α-tublin (T5168, Sigma), and SC35 (S4045, Sigma).

Immunopurification of the WTAP Complexes from the Whole Cell Lysate of HUVEC, HEK293, and HeLa Cells—Cells were grown to 75–80% confluence in a 150-mm dish, harvested, suspended in 1 ml of lysis buffer (20 mM HEPES (pH 7.9), at 4 °C, 10% glycerol, 250 mM KCl, 0.2 mM EDTA, 0.1% Nonidet P-40, 0.2 mM PMSF) with protease inhibitors (Roche Applied Science) and 50 units of Benzonase (Novagen), and then incubated on ice for 30 min. After centrifugation for 30 min at 12,000 × *g* at 4 °C, the supernatant was frozen with liquid nitrogen and stored at −80 °C as the cell lysate. Immunopurification was performed with 2 μg of antibody-cross-linked Dynabeads protein G (Invitrogen), as described previously (24).

Cross-linking and Immunopurification—HeLa cells were cross-linked with 1% paraformaldehyde for 10 min. After neutralization with 0.2 M glycine, cells were collected, resuspended in SDS lysis buffer (10 mM Tris-HCl, 150 mM NaCl, 1% SDS, 1 mM EDTA (pH 8.0), RNase inhibitor, protease inhibitor mixture), and fragmented with a sonicator (Sonifier 250, Branson; 4 min, 60% duty, output level 4). The sonicated solution was diluted with 3 volumes of dilution buffer (20 mM Tris-HCl (pH 8.0), 150 mM NaCl, 1 mM EDTA, 1% Triton X-100) and was used for immunoprecipitation with the H1122 antibody-conjugated magnetic beads. The immunoprecipitates were eluted in elution buffer (50 mM Tris-HCl (pH 8.0), 10 mM EDTA, 1% SDS) at 65 °C for 15 min and then concentrated with methanol/chloroform, washed with ice-cold acetone, and dried.

Liquid Chromatography-Tandem Mass Spectrometry (LC/MS/MS)—The immunopurified (IP) samples were subjected to in-solution trypsin digestion followed by LC/MS/MS using an LTQ Orbitrap XL ETD mass spectrometer (Thermo Scientific), as described previously (25). All of the MS/MS samples were analyzed using Mascot (version 2.4.0; Matrix Science, London, UK). Mascot was set up to search against the human Swiss-Prot database assuming a digestion with trypsin. The fragment and parent ion mass tolerances were 0.8 Da and 3 ppm, respectively. Three missed cleavages were allowed. The analysis of the data was carried out with Scaffold software (version 3; Proteome Software Inc., Portland, OR). Peptide identifications were only accepted if they could be established at >95.0% probability.

Generation of the Hakai Expression Vector and Stable Cell Lines—The Hakai coding sequence was subcloned into a pCMV2-FLAG vector (Sigma). Hakai deletion mutants for the RING finger and phosphotyrosine binding region were constructed by mutagenesis. For stable cell line generation, we used a Hakai truncated mutant (aa 1–417) having a V5 sequence at the C terminus (Hakai-V5), which can interact with WTAP, because full-length Hakai was not sufficiently expressed. A RING finger deletion mutant (Hakai-delRING-V5) was also constructed using mutagenesis. Dox-inducible HEK293 stable cells expressing Hakai-V5 and Hakai-delRING-V5 were generated using the Flp-In™ T-REx™ core kit (Invitrogen) according to the manufacturer's protocol. 100 ng/ml doxycycline (BD Biosciences) was used for the induction.

siRNA Transfection—siRNAs against WTAP, Virilizer, BCLAF1, THRAP3, KIAA0853, Hakai, and RBM15 as well as negative control siRNA were purchased from Ambion (s18433, s24832, s18875, s19360, s23010, s36537, and s224626, respectively). These siRNAs were transfected with Lipofectamine

2000 RNAi MAX (Invitrogen) according to the manufacturer's protocol.

Fluorescence Image Analysis—Cells were fixed with 4% (w/v) paraformaldehyde in PBS for 5 min, permeabilized with 0.5% (v/v) Triton X-100 in PBS for 5 min on ice, blocked with PBS containing 10% BlockAce (Yukijirushi, Japan), and incubated with the primary antibodies against WTAP (1:200; rabbit polyclonal antibody, 1:100; Y6828), SC-35 (1:2000; S4045, Sigma), BCLAF1 (1:100; A300-608A, Bethyl), THRAP3 (1:200; A300-956A, Bethyl), Virilizer (1:250; A302-124A, Bethyl), KIAA0853 (1:100; ab70802, Abcam), Hakai (1:80; ARP39623_T100, Aviva Systems Biology), and RBM15 (1:80; ab70549, Abcam) for 30 min at room temperature. Alexa Fluor 488 anti-mouse IgG (1:500; Invitrogen) and Alexa Fluor 594 anti-rabbit IgG (1:500; Invitrogen) were used as secondary antibodies. Cells were mounted in Prolong Gold Antifade Reagent (Invitrogen) with DAPI nuclear staining except for the immunofluorescence of Hakai-WT-V5 and Hakai-delRING-V5, where TO-pro3 was used for nuclear staining. RNA FISH was performed according to the protocol reported by Tripathi *et al.* (26). To detect MALAT1 RNA, cells were rinsed briefly in PBS and then fixed in 4% formaldehyde in PBS (pH 7.4) for 15 min at room temperature. The cells were permeabilized in PBS containing 0.5% Triton X-100 and 5 mM VRC (New England Biolabs) on ice for 10 min, washed with PBS 3 × 10 min, and rinsed once in 2× SSC prior to hybridization. Hybridization was carried out using a nick-translated cDNA probe (Abbott Molecular) in a moist chamber at 37 °C for 12–16 h according to the manufacturer's instructions. After RNA-FISH, cells were again fixed for 10 min in 2% paraformaldehyde, and immunofluorescence staining was performed as described above. Fluorescence images were acquired with a confocal laser-scanning microscope (IX81/FV1000, Olympus) using a ×100, 1.40 numerical aperture objective or a confocal laser-scanning microscope (LSM510META, Carl Zeiss), and the images were processed using ImageJ (National Institutes of Health) and Zeiss 3D software. Quantification of the colocalization coefficients, derived from the measured pixel overlaps between WTAP or MALAT1 and SC35, was performed with Zeiss LSM510 META colocalization analysis software using 20 independent single-cell images.

RNA Co-immunoprecipitation (RIP) and Quantitative RT-PCR—RIP was performed based on a ChIP protocol. HUVECs were trypsinized, centrifuged, and washed with PBS. Cells were resuspended in 5 volumes of hypotonic buffer (10 mM HEPES (pH 7.9) at 4 °C, 1.5 mM $MgCl_2$, 10 mM KCl, 0.2 mM PMSF, protease inhibitor mixture, RNAsin) and incubated for 10 min on ice. Suspended cells were homogenized by eight passages through a 21-gauge needle, and the nuclei were collected by centrifugation for 15 min at 3000 rpm and cross-linked with 4% paraformaldehyde in PBS for 10 min. After neutralization with 0.2 M glycine, cells were collected, resuspended in SDS lysis buffer (10 mM Tris-HCl, 150 mM NaCl, 1% SDS, 1 mM EDTA (pH 8.0), protease inhibitor mixture, RNAsin), and sonicated (Sonifier 250, Branson; 4 min, 60% duty, output level 4). The sonicated solution was diluted with ChIP dilution buffer (20 mM Tris-HCl (pH 8.0), 150 mM NaCl, 1 mM EDTA, 1% Triton X-100) and used for IP, and 1% of the starting materials were used as the input. An anti-WTAP antibody (H1122) bound with Protein G magnetic beads was used. After IP, samples were reverse cross-linked, total RNA was extracted using TRIzol LS (Invitrogen) and treated with RNase-free DNase I (Promega), and then RT-PCR was conducted using random hexamer primers following the manufacturer's instructions (Invitrogen).

RNase Protection Assay—The RNase protection assay was performed using an RPAIII ribonuclease protection assay kit (Ambion) according to the manufacturer's protocol. The WTAP cDNA fragment was amplified from the total HUVEC RNA by RT-PCR. The amplified cDNA was cloned into the pCRII vector (Invitrogen), verified by sequencing, and used as the template for a riboprobe.

Statistical Analysis—All experiments were performed a minimum of three times. Data points represent the mean ± S.D. calculated from multiple independent experiments. Statistically significant differences were calculated by using either the unpaired *t* test or analysis of variance and Tukey-Kramer multiple comparison tests with Statcel3 software (OMS Publishing Inc., Saitama, Japan). *p* values less than 0.05 were considered significant.

All of the primers used in this study are listed in supplemental Table S2.

RESULTS

Identification of the WTAP Complex Components—To characterize the role of WTAP in the cellular machinery, we purified WTAP and its interacting proteins from HUVEC extracts by immunopurification using three specific monoclonal antibodies against human WTAP and performed shotgun proteomics. We generated three monoclonal antibodies. H1122 and H1137 recognize the C terminus of the human WTAP protein, whereas Y6828 was generated against the N-terminal sequence of the human WTAP protein corresponding to aa 1–50 (Fig. 1*A*; see "Experimental Procedures"). The specificity for WTAP was tested by immunoblotting (Fig. 1*B*). Endogenous WTAP corresponding to a ~50 kDa band was detectable by all three antibodies and disappeared after WTAP knockdown with siRNA against WTAP. These antibodies were conjugated to protein G magnetic beads and used for immunopurification.

The immunopurification of the native protein complexes was based on a highly sensitive immunoprecipitation system (24). WTAP was immunoprecipitated effectively by each antibody but not with the antiviral protein antibody K7124, which was used as a negative control (Fig. 1*C*). The nonspecific bands observed in the immunoblot performed with H1137 (Fig. 1*B*) were undetectable in the immunoprecipitates obtained with H1137 (data not shown). From the results of the protein staining of the purified fractions, the purification quality was regarded as sufficient to carry out shotgun proteomics (Fig. 1*C*). The proteins in the immunoprecipitates were digested in solution, and the resulting peptides were identified using high performance liquid chromatography combined with tandem mass spectrometry (LC/MS/MS). WTAP was identified with approximately a 70% sequence coverage in all three samples (supplemental Table S1). The overlapping binding candidates that were isolated with all three of the anti-WTAP antibodies, but not with the negative control antibody K7124, included the

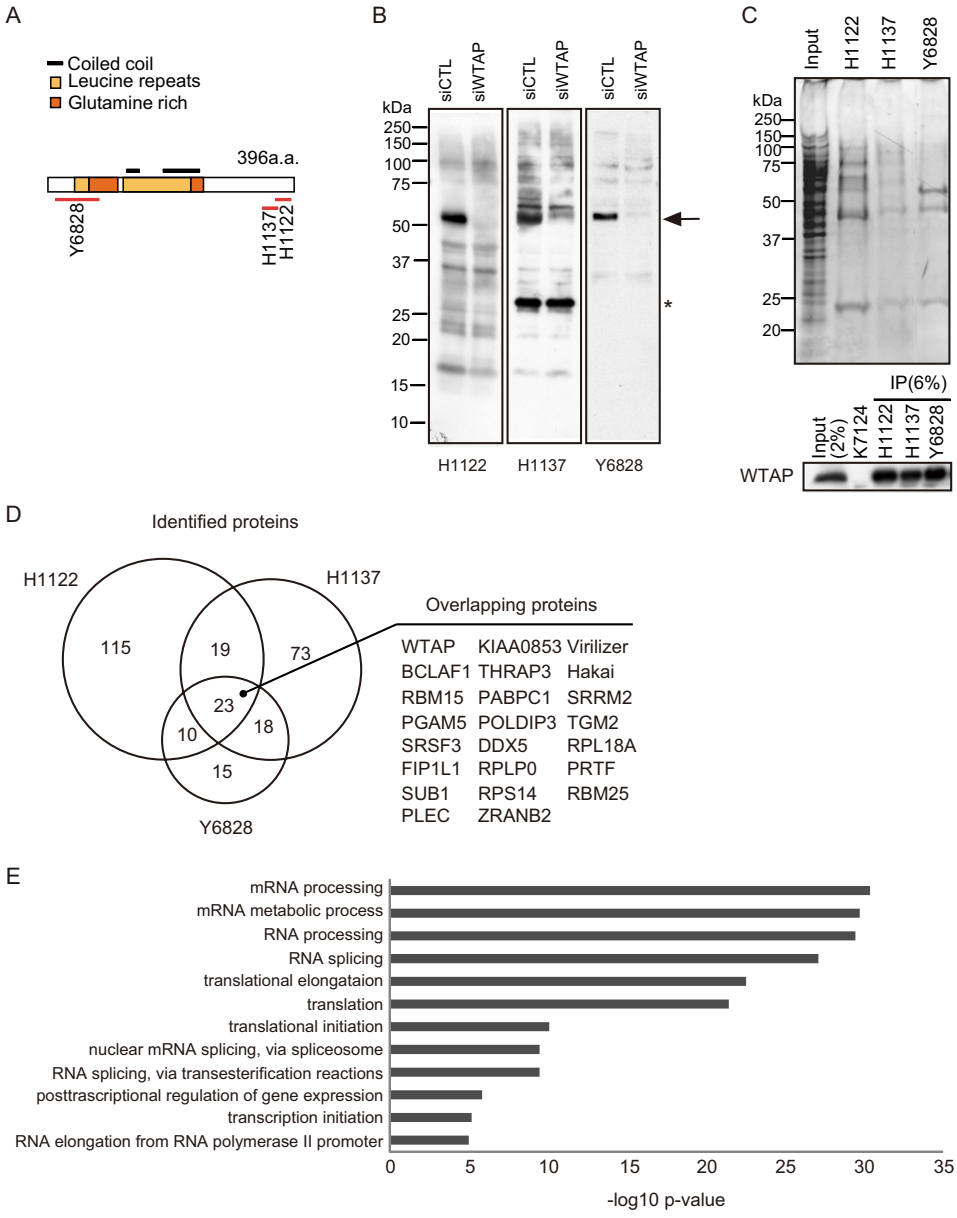

FIGURE 1. **Immunopurification of the WTAP binding proteins using three anti-WTAP monoclonal antibodies.** *A*, three specific monoclonal antibodies against WTAP were generated. The recognition region of each antibody is indicated with a *heavy line*. *B*, specificity of anti-WTAP antibodies. Whole lysates of HUVECs were subjected to immunoblot analysis using H1122 and H1137 antibodies, whereas nuclear extracts were used for Y6828. The *arrow* indicates the band corresponding to WTAP, which is undetectable in WTAP siRNA-treated HUVECs. The *asterisks* represent nonspecific or cross-reactive bands. *C*, immunopurified (*IP*) WTAP and its interacting proteins from HUVECs were stained with SYPRO Ruby and immunoblotted with an anti-WTAP polyclonal antibody. *D*, Venn diagram of the number of proteins isolated with at least three unique peptides by the anti-WTAP antibodies H1122, H1137, and Y6828 but not with the negative control anti-viral protein antibody K7124. The overlapping proteins that were isolated by all three of the anti-WTAP antibodies are indicated. *E*, gene ontology analysis of the proteins isolated with at least three unique peptides by the anti-WTAP antibodies H1122, H1137, and Y6828 but not the anti-gp64 antibody. The significant enrichment of functional biological processes is shown along with the *p* value.

Virilizer homolog, zinc finger protein KIAA0853, Hakai, mRNA export cofactor RBM15, and the SR-like proteins BCLAF1 and THRAP3 (Fig. 1*D*). *Vir* has been reported to interact with *fl(2)d* both genetically and physically in *Drosophila* (10, 12, 13). The presence of Virilizer homolog in the purified fractions verified the biological relevance of the WTAP complex. Gene ontology analysis of the identified proteins revealed a high level of enrichment of the interacting proteins in terms of RNA processing, such as RNA splicing and translation (Fig. 1*E*). These proteins were also isolated in experiments using HeLa cells with an H1122 antibody (supplemental Table S1), indicating that these complexes are not exclusive to HUVECs.

We next examined the interaction between WTAP and one of the interaction candidates, Hakai (also known as CBLL1), which is a C3HC4-type RING finger containing E3 ubiquitin ligase that mediates ubiquitination of the E-cadherin complex (27). In addition to its role in cell-cell contact, Hakai has recently been shown to promote cell proliferation in *Drosophila* embryo (28) and mammalian cells and to enhance the RNA-binding ability of polypyrimidine tract-binding protein-associ-

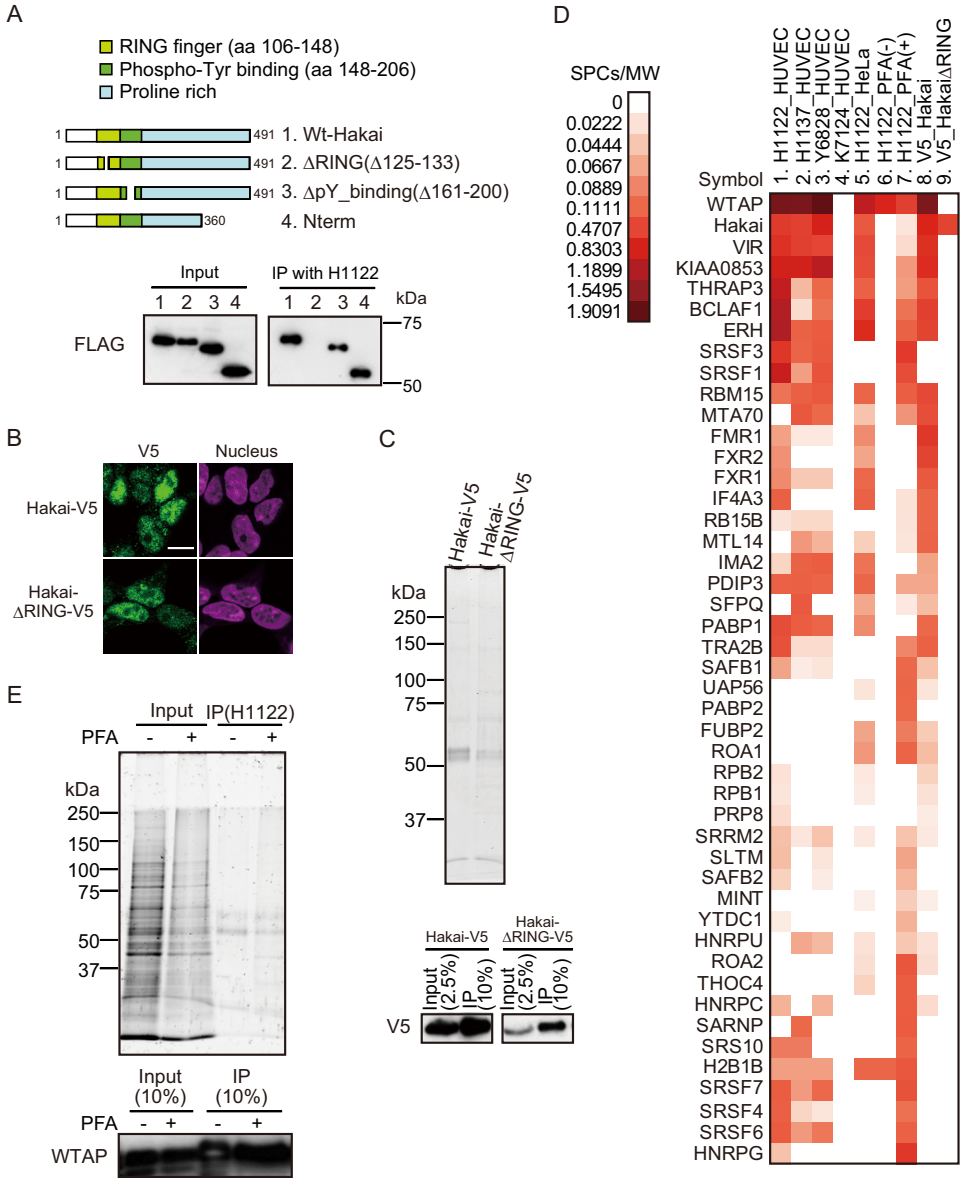

FIGURE 2. **Proteomic profile of the WTAP complexes.** *A*, the domains and unique amino acid repeats in the Hakai protein. Various Hakai deletion mutants are shown. The interaction of these mutants with WTAP was assessed by means of co-immunoprecipitation (*IP*) experiments. *B*, the cellular localization of Hakai-V5 and Hakai-delRING-V5. The nucleus was stained with TO-PRO-3 reagent. *Bar*, 10 μm. *C*, immunoprecipitation of Hakai complexes from the tetracycline-inducible HEK293 stable cell lines expressing Hakai-V5 or Hakai-delRING-V5. Immunopurified Hakai and its interacting proteins were resolved by SDS-PAGE and stained with SYPRO Ruby solution. The efficiency of immunoprecipitation was determined by Western blot. *D*, the proteomic profile of the WTAP complexes. This list shows the proteins isolated using the H1122, H1137, or Y6828 antibodies with a unique peptide number of ≥3 from HUVEC extracts or from PFA(+) HeLa cell extracts but not with the negative control antibody K7124 from HUVEC extracts or the anti-V5 antibody from the Hakai-delRING-V5 sample. The complete list of the identified proteins is presented in supplemental Table S1. The values represent the unweighted spectrum count (*SPC*) level divided by the molecular weight (*MW*) in kDa to determine the relative quantity of the immunopurified proteins. Hierarchical clustering was performed using JMP 7 software (SAS Institute, Cary, NC). *E*, immunopurification of the proteins cross-linked to WTAP. HeLa cells were cross-linked with paraformaldehyde, and the proteins cross-linked to WTAP were immunopurified with the H1122 antibody. Interacting proteins were resolved by SDS-PAGE and stained with SYPRO Ruby solution.

ated splicing factor (29). Hakai contains a RING finger (aa 106–148) and a phosphotyrosine-binding domain (aa 148–206) called the Hakai Tyr(P)-binding (HYB) domain, as characterized by biochemical and crystal structural analyses (30), and a proline-rich domain in the C terminus. The RING finger domain of Hakai is required for the regulation of cell proliferation (29). Thus, the interaction of Hakai with WTAP was confirmed using the Hakai mutants (Fig. 2*A*). The use of several different Hakai mutants showed that the Hakai mutant lacking the RING finger (*i.e.* Hakai-delRING) did not interact with WTAP (Fig. 2*A*), suggesting that the interaction between WTAP and Hakai is involved in cell cycle regulation.

We next generated tetracycline-inducible HEK293 stable cell lines expressing a V5-tagged Hakai or Hakai-delRING, respectively, and confirmed the nuclear localization of both proteins (Fig. 2*B*). Then we isolated the interacting proteins using an anti-V5 antibody (Fig. 2*C*). Interestingly, WTAP and its interacting proteins that were mentioned above, such as Virilizer, KIAA0853, BCLAF1, THRAP3, RBM15, FMR1, FXR1, FXR2, and MTA70 (N^6-adenosine methyltransferase 70-kDa sub-

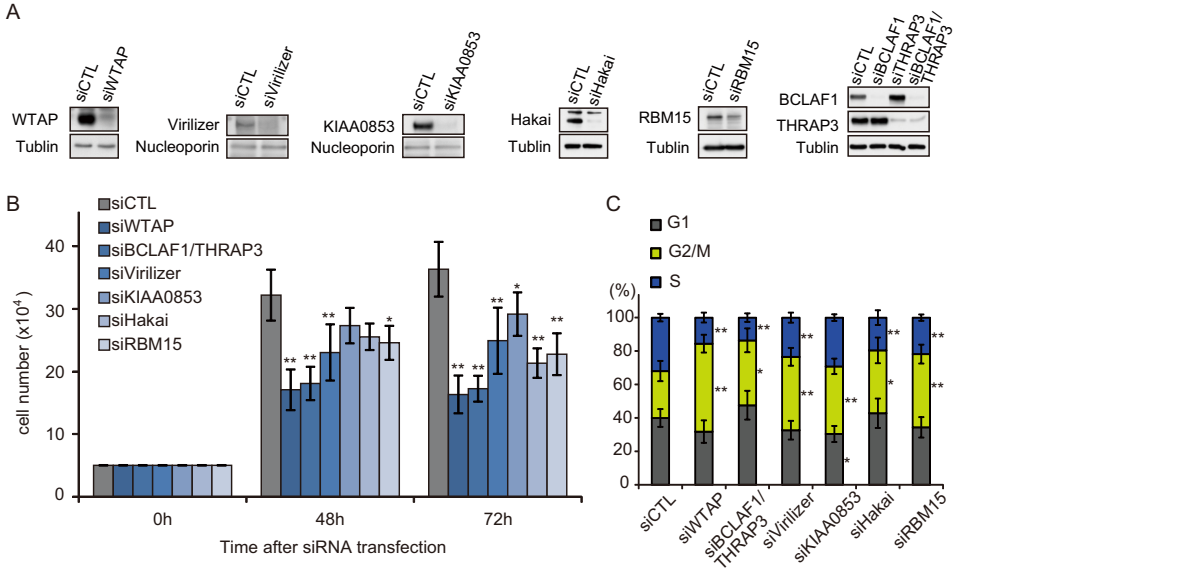

FIGURE 3. **The effect of the depletion of each component of the WTAP complex on cell proliferation.** *A*, the efficiency of RNAi was confirmed by Western blot using whole cell extracts except for the detection of the Virilizer and KIAA0853 proteins, for which nuclear extract was used to detect the endogenous proteins. α-Tublin or nucleoporin was used as a loading control. *B*, effect of the depletion of Hakai, Virilizer, KIAA0853, RBM15, or BCLAF1/THRAP3 on cell proliferation. The values are the average of six independent experiments. *C*, the cell cycle profile was analyzed using FACScalibur. Forty-eight hours after siRNA transfection, cells were harvested and stained with propidium iodide for DNA content determination. The values are the average ± S.D. (*error bars*), $n = 10$. For *B* and *C*, **, $p < 0.01$; *, $p < 0.05$ *versus* control (Tukey-Kramer post hoc test).

unit), were isolated using Hakai-V5 but not with Hakai-delRING-V5 (compare *columns 8* and *9* in Fig. 2*D* and supplemental Table S1). This shows that WTAP and its interacting proteins form a complex with Hakai through the RING finger domain.

The WTAP Complex Transiently Interacts with General Splicing Regulators—Recent studies have shown that a combination of chemical cross-linking, affinity purification, and mass spectrometry analysis provides a direct method of determining stable, weak, or transient protein-protein interactions with high confidence (31, 32). Formaldehyde has been routinely used as an effective cross-linker that forms covalent bonds between proteins, nucleic acids, and other reactive molecules. In an effort to capture the more transient protein-protein and/or RNA-dependent interactions, we purified WTAP-interacting proteins from HeLa cells with the H1122 antibody after paraformaldehyde cross-linking (Fig. 2*E*). The purified complexes were reverse cross-linked and identified by shotgun proteomics. General splicing regulators, including heterogeneous nuclear ribonucleoprotein, SR proteins, and small nuclear ribonucleoproteins as well as the proteins described above, were enriched among the proteins cross-linked to WTAP (Fig. 2*D*, *columns 5* and *7*, and supplemental Table S1), whereas only WTAP was identified from the cross-linked (−) IP fraction, due to a series of stringent washing steps (compare *columns 6* and *7* in Fig. 2*D*). These results indicate a transient and/or RNA-dependent interaction of WTAP with the splicing machinery.

The WTAP Complex Is Required for Cell Proliferation—We next examined the effect of the respective depletion of the major components Hakai, Virilizer, KIAA0853, BCLAF1, THRAP3, and RBM15 on cell proliferation in HUVECs. BCLAF1 and THRAP3 were depleted together due to their sequence similarity and possible functional redundancy (Fig. 3*A*). We have shown previously that WTAP reduction leads to growth inhibition and G_2 phase accumulation in the cell cycle (17). As shown in Fig. 3*B*, control siRNA-treated cells grew moderately for the first 48 h after siRNA transfection and then increased 7-fold in cell number by 72 h. In contrast, WTAP, Hakai, Virilizer, KIAA0853, RBM15, or BCLAF1/THRAP3 siRNA-treated cells exhibited growth inhibition, as evidenced by the evidently reduced increase in cell number. Moreover, flow cytometric analysis revealed that WTAP, Hakai, Virilizer, KIAA0853, RBM15, or BCLAF1/THRAP3 siRNA-treated cells exhibited a significantly higher proportion in the G_2 phase than control cells (Fig. 3*C*), providing further evidence of their functional relationship in cell cycle regulation.

WTAP Localizes to Nuclear Speckles through an Interaction with BCLAF1/THRAP3—The SR-like proteins BCLAF1/THRAP3 as well as WTAP have been shown to reside in interchromatin granule clusters (16) and also in affinity-purified mRNP complexes (33). Thus, we examined the cellular localization of WTAP and BCLAF1/THRAP3 by immunofluorescence analysis. When HUVECs were stained with an anti-WTAP antibody (Y6828), a strong signal was observed in the nuclear speckles as well as the nucleoplasm (Fig. 4*A*). The speckle distribution pattern was overlapped with the nuclear speckle marker SC35. Similar results were obtained from the immunofluorescence using an anti-BCLAF1 or anti-THRAP3 antibody together with anti-SC35 (Fig. 4*A*). Furthermore, we examined the cellular localization of the other components of the complex and found that Virilizer, KIAA0853, Hakai, and RBM15 also localize to nuclear speckles and the nucleoplasm (Fig. 4*A*). Next we confirmed the colocalization of WTAP and BCLAF1 or THRAP3 in the nucleoplasm and nuclear speckles (Fig. 4*B*). Then we examined the effect of the depletion of BCLAF1 and THRAP3 on the localization of WTAP. Interestingly, we found that the depletion of BCLAF1 and THRAP3 resulted in a decreased nuclear speckle distribution of WTAP

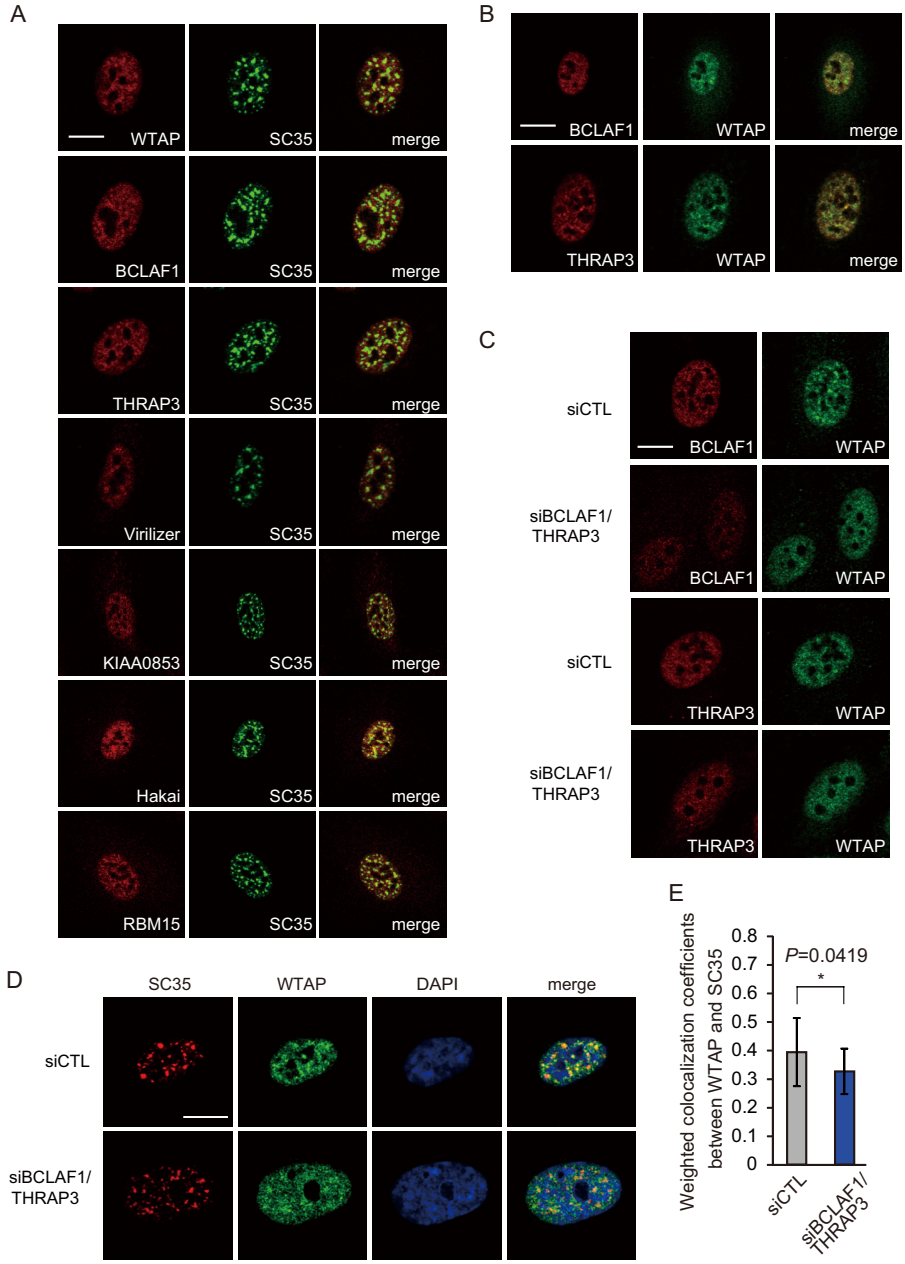

FIGURE 4. **The intracellular localization of the WTAP complex.** *A*, immunofluorescence analysis of HUVEC using anti-WTAP (rabbit polyclonal antibody), anti-BCLAF1, anti-THRAP3, anti-Virilizer, anti-KIAA0853, anti-Hakai, anti-RBM15, and anti-SC35 antibodies. WTAP, BCLAF1, THRAP3, Virilizer, KIAA0853, and RBM15 are all partially co-localized with SC35 in nuclear speckles and are also present in the nucleoplasm. *B*, the intracellular localization of WTAP (Y6828), BCLAF1, and THRAP3. WTAP is co-localized with BCLAF1 and THRAP3 in nuclear speckles and the nucleoplasm. *C*, the nuclear speckle localization of WTAP became dispersed upon knockdown of BCLAF1/THRAP3. HUVECs were treated with BCLAF1/THRAP3 siRNAs or control siRNA and, after 48 h, immunostained with an anti-WTAP antibody (Y6828) together with anti-BCLAF1 or anti-THRAP3 antibodies. The WTAP signal became evidently more dispersed in BCLAF1/THRAP3 knockdown cells compared with the signal in control cells. *D*, confocal images of WTAP (rabbit polyclonal antibody) and SC35 in control or BCLAF1/THRAP3 siRNA-treated HUVECs. The DNA is counterstained with DAPI (*blue*). *E*, the quantification of the colocalization coefficient between WTAP and SC35. The values are the average of 20 independent single-cell images. *, $p < 0.05$ (*t* test). *Error bars*, S.D. *Bar*, 10 μm.

(Fig. 4*C*), although the nuclear speckles were still present, as indicated by the speckle localization of SC35 (Fig. 4*D*). Colocalization analysis using Zeiss LSM510 META colocalization analysis software also confirmed the reduced speckle localization of WTAP by BCLAF1/THRAP3 depletion (Fig. 4*E*). These findings indicate that BCLAF1/THRAP3 facilitates the nuclear speckle localization of WTAP. Nuclear speckles are highly dynamic subnuclear domains enriched with pre-mRNA splicing/processing factors (34) and the long nuclear-retained regulatory RNA, MALAT1 (35, 36). It has been reported that MALAT1 modulates the distribution and phosphorylation of splicing factors in nuclear speckles and regulates alternative splicing and cell cycle progression (26, 37, 38). To examine the interaction between WTAP and MALAT1, we performed RIP analysis using the anti-WTAP antibody H1122 followed by quantitative PCR. Significant enrichment of MALAT1 in the immunoprecipitates treated with H1122 was observed, indicating that WTAP interacts with MALAT1 (Fig. 5*A*). We further

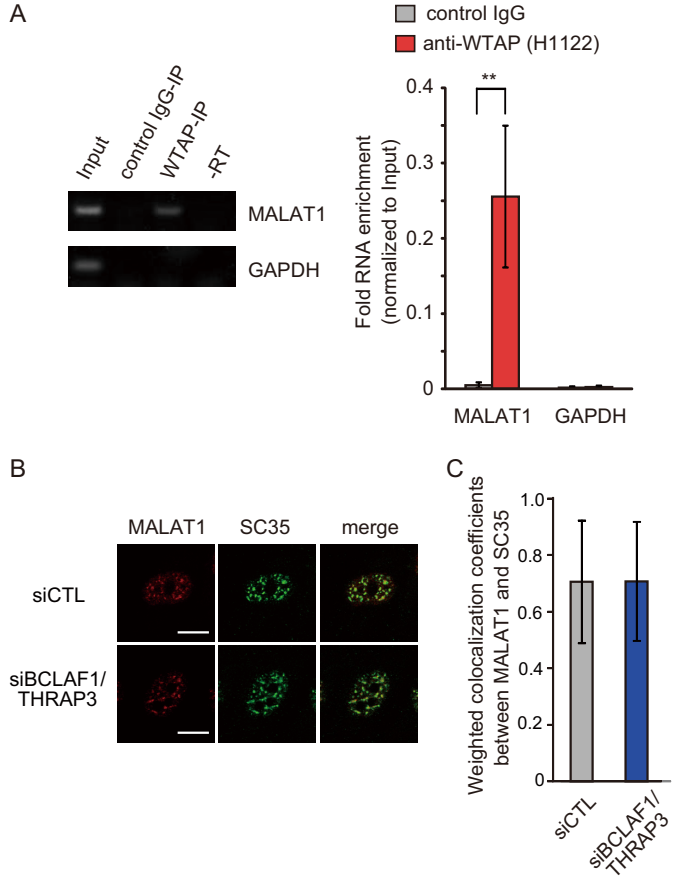

FIGURE 5. **The interaction of WTAP and the noncoding RNA MALAT1.** *A*, a representative gel image of RT-PCR from the RIP samples using MALAT1- or GAPDH-specific primers (*left*). The interaction of WTAP with MALAT1 was determined by RIP-quantitative PCR (*right*). GAPDH was used as a negative control. The values are the average of five independent experiments; *, $p <$ 0.05 (*t* test). *Error bars*, S.D. *B*, RNA-FISH and immunostaining were performed using a probe against MALAT1 and an anti-SC35 antibody in the control or BCLAF1/THRAP3 siRNA-treated HUVECs. *Bar*, 10 μm. *C*, the quantification of the colocalization coefficient between MALAT1 and SC35. The values are the average of 20 independent single-cell images. *Error bars*, S.D.

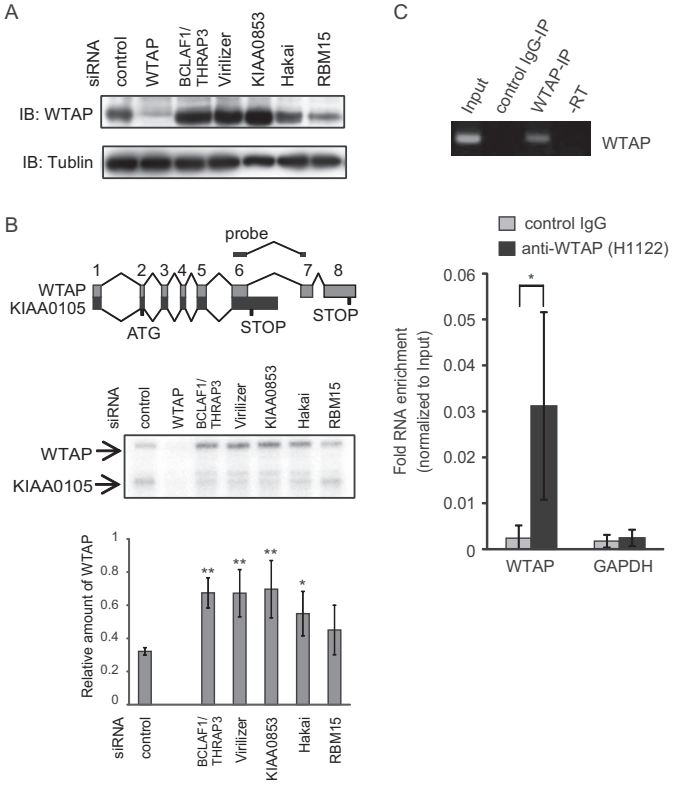

FIGURE 6. **The WTAP complex autoregulates the alternative splicing of *WTAP* pre-mRNA.** *A*, Western blot analysis of the WTAP protein. In the course of the depletion of the WTAP complex proteins, the protein level of WTAP was increased compared with control cells. α-Tublin was used as a loading control. We did not detect the shorter isoform of the endogenous WTAP protein despite the application of several specific antibodies. *B*, the effect of the depletion of each protein in the WTAP complex on the *WTAP* transcript was determined by RNase protection assay. The region used for the probe is indicated. **, $p < 0.01$; *, $p < 0.05$ (*t* test), $n = 4$. *C*, representative gel image of RT-PCR from the RIP samples using WTAP-specific primers (*top*). The interaction of WTAP with *WTAP* pre-mRNA was determined by RIP-quantitative PCR (*bottom*). GAPDH was used as a negative control (the same data as in Fig. 5*A*). The values are the average of five independent experiments; *, $p < 0.05$ (*t* test). *Error bars*, S.D. *IB*, immunoblot.

examined the nuclear localization of MALAT1 by RNA-FISH in the presence or absence of BCLAF1/THRAP3. As shown in Fig. 5*B*, MALAT1 was detected in the nuclear speckles with SC35 and the nucleoplasm in control cells, consistent with a previous report (37). Unlike WTAP, the speckle distribution of MALAT1 was unchanged upon the knockdown of BCLAF1/THRAP3 (Fig. 5, *B* and *C*).

The WTAP Complex Autoregulates Alternative Splicing of WTAP Pre-mRNA—While investigating the effect of the depletion of WTAP-interacting proteins by siRNA, we found that WTAP protein expression was up-regulated in BCLAF1/THRAP3, Virilizer, KIAA0853, and Hakai siRNA-treated cells (Fig. 6*A*). WTAP has two transcript variants due to alternative splicing and alternative polyadenylation, one of which encodes the shorter isoform, ending just after exon 6, referred to as KIAA0105. It includes the retained sequences of intron 6, leading to a "bleeding" exon with immediate translation termination. The stop codon is skipped when the 3′ splice site of exon 6 is used, generating an mRNA that encodes the full-length WTAP protein (Fig. 6*B*). To determine whether the up-regulation of WTAP protein expression was due to alternative splicing, we performed RNase protection analysis using riboprobes that were able to detect the isoforms separately. Both the shorter isoform (~70%) and longer isoform (~30%) were present in control cells (Fig. 6*B*). The BCLAF1/THRAP3, Virilizer, KIAA0853, and Hakai siRNA-treated cells displayed a significantly higher ratio of the longer isoforms compared with the control cells ($p < 0.05$), suggesting that the WTAP complex acts as a repressor of *WTAP* gene splicing in a concentration-dependent manner, and the resulting splicing alteration is probably responsible for the up-regulation of WTAP protein expression in the cells depleted of each of the respective proteins in the complexes. To examine the interaction between WTAP and *WTAP* pre-mRNA, we performed RIP analysis. Significant enrichment of WTAP in the immunoprecipitates with H1122 was observed (Fig. 6*C*, $p < 0.05$), suggesting the direct regulation of alternative splicing of WTAP pre-mRNA by the complex.

DISCUSSION

In the present study, we identified the WTAP complex, which is involved in RNA processing and cell cycle, using a

highly sensitive shotgun proteomics. To detect the intrinsic complex, we generated several monoclonal antibodies against WTAP. The three clones we used in the present study recognize the N-terminal or C-terminal portions of the WTAP protein, which could compensate for any loss of a complex by one clone due to a covering of the epitope by binding proteins. The specificity of the interaction with WTAP was further supported by the observation that WTAP and its interacting proteins were isolated with Hakai-V5 but not with Hakai-delRING-V5. This also probably indicates that these proteins form a large complex with WTAP and act as the complex. From the results of serial proteomic analyses using HUVECs with three monoclonal antibodies, HeLa cells, and HEK293 cells expressing Hakai-V5 or Hakai-delRING-V5, it was determined that Virilizer, KIAA0853, Hakai, BCLAF1, THRAP3, and RBM15 are the major components of the WTAP complex (Fig. 2*D*).

In addition, we demonstrated a transient interaction of the WTAP complexes with the splicing machinery using a combined cross-linking and immunopurification method. This method was confirmed to be effective in both purifying a protein of interest and also identifying the transiently associated protein complexes in cultured mammalian cells. From these proteomic analyses, the binding candidates to WTAP also include FMRP, the FMR1 (fragile X mental retardation 1) gene product, and its autosomal paralogues, FXR1 and FXR2 (fragile X mental retardation syndrome-related protein 1 and 2, respectively), ERH (enhancer of rudimentary homologue), and MTA70 (Fig. 2*D*). Fragile X syndrome, the most common heritable X-linked neurodevelopmental disorder, is caused by the loss of function of FMRP. FMRP has been implicated in translational control, associating with actively translating polyribosomes in ribonucleoprotein particles (reviewed in Ref. 39). ERH is a highly conserved protein that has been implicated in nuclear gene expression (40, 41) and cell growth (42–44). Recent studies have reported that ERH-depleted cells show severe chromosome misalignment with a loss of kinetochore localization of CENP-E (centromere-associated protein E) (45, 46). ERH interacts with spliceosome proteins and is required for the mRNA splicing of CENP-E (45). MTA70 is the *S*-adenosylmethionine-binding subunit of human mRNA:m(6)A methyltransferase, an enzyme that sequence-specifically methylates adenines in pre-mRNA. The biological significance of this modification remains unclear. Interestingly, plant MTA is potently expressed in dividing tissues and has been shown to bind to FIP37, a plant homologue of WTAP (47). Thus, in addition to mRNA stabilization and alternative splicing regulation, our proteomic data suggest that WTAP dynamically takes part in several posttranscriptional processes by forming a protein complex with these components.

We further demonstrated the interaction of WTAP and the non-coding RNA MALAT1 by RIP analysis. The interaction of WTAP with MALAT1 may contribute to the formation and/or modification of the complex in nuclear speckles. Upon the knockdown of BCLAF1/THRAP3, the nuclear speckle localization of WTAP became dispersed, whereas the speckle distribution of MALAT1 persisted. It is possible that the interaction of WTAP with MALAT1 may be reduced in the absence of BCLAF1/THRAP3.

It has been proposed that RNA processing is associated with cell cycle regulation, as demonstrated by the fact that several pre-mRNA splicing mutants (prp) from temperature-sensitive *Schizosaccharomyces pombe* strains have cell division cycle defects (48). A growing body of evidence has indicated a functional connection between RNA splicing and cell cycle regulation (49–51). Although the precise mechanisms mediating the role of splicing and/or spliced variants in the cell cycle are not well understood, it is believed that specific splicing factors are involved in the control of the splicing of cell cycle-related genes, especially the alternative splicing of apoptotic regulators (52) and/or genomic stability (53). The prototypic SR protein splicing factor SF2/ASF is up-regulated in various human tumors and is a potent oncoprotein, whose overexpression by as little as 2-fold is sufficient to transform rodent fibroblasts (51). Conversely, the knockdown of SF2/ASF induces G_2 cell cycle arrest and apoptosis, presumably through the accumulation of DNA double strand breaks (54). Similarly, the loss of the SR protein SC35 in mouse embryonic fibroblasts induces G_2/M cell cycle arrest and genomic instability (55). Moreover, it is reported that SRp20 and polypyrimidine tract-binding protein are highly expressed in epithelial ovarian cancer, and the knockdown of those factors leads to growth arrest and apoptosis (50). We demonstrated that the depletion of each of the respective WTAP complex components, namely WTAP, Virilizer, KIAA0853, BCLAF1/THRAP3, Hakai, and RBM15, resulted in cell cycle arrest at G_2 phase, suggesting that the responsible mechanism for the cell cycle progression is carried out by this protein complex. Genome instability was not observed in WTAP knockdown cells examined with immunofluorescence of phosphorylated γH2AX to detect induced foci that had accumulated on broken DNA (data not shown).

In the regulation of *WTAP* transcripts by the WTAP complex, the data indicate that the WTAP complex probably prevents the 3′ splicing of intron 6 and/or promotes alternative polyadenylation of intron6 so as to produce a shorter isoform that does not encode the full-length protein, thereby negatively controlling the *WTAP* protein expression. In *Drosophila*, SXL regulates the splicing of *Sxl* (56–58), *tra* (7, 59, 60), and *msl-2* RNA (61, 62) via a blockade that occurs by binding to the poly(U) sequences present at the 5′ splice site and/or the polypyrimidine tract of the 3′ splice site. There might be such a mechanism that is conserved in *Drosophila* and mammals in the alternative splicing regulation effected by WTAP.

In conclusion, we have identified and characterized the WTAP complex, which is involved in both alternative splicing and cell cycle regulation. Additional studies, such as a comprehensive analysis of the binding sites for the complex in RNA transcripts, will help to elucidate the detailed molecular mechanisms of the alternative splicing and cell cycle regulation carried out by the WTAP complex.

Acknowledgment—We thank Dr. Kevin Boru of Pacific Edit for review of the manuscript.

REFERENCES

1. Kalsotra, A., and Cooper, T. A. (2011) Functional consequences of developmentally regulated alternative splicing. *Nat. Rev. Genet.* **12,** 715–729

2. Venables, J. P., Klinck, R., Koh, C., Gervais-Bird, J., Bramard, A., Inkel, L., Durand, M., Couture, S., Froehlich, U., Lapointe, E., Lucier, J. F., Thibault, P., Rancourt, C., Tremblay, K., Prinos, P., Chabot, B., and Elela, S. A. (2009) Cancer-associated regulation of alternative splicing. *Nat. Struct. Mol. Biol.* **16,** 670–676
3. Wang, E. T., Sandberg, R., Luo, S., Khrebtukova, I., Zhang, L., Mayr, C., Kingsmore, S. F., Schroth, G. P., and Burge, C. B. (2008) Alternative isoform regulation in human tissue transcriptomes. *Nature* **456,** 470–476
4. Nagoshi, R. N., McKeown, M., Burtis, K. C., Belote, J. M., and Baker, B. S. (1988) The control of alternative splicing at genes regulating sexual differentiation in *D. melanogaster*. *Cell* **53,** 229–236
5. Bashaw, G. J., and Baker, B. S. (1995) The msl-2 dosage compensation gene of *Drosophila* encodes a putative DNA-binding protein whose expression is sex specifically regulated by Sex-lethal. *Development* **121,** 3245–3258
6. Bell, L. R., Horabin, J. I., Schedl, P., and Cline, T. W. (1991) Positive autoregulation of sex-lethal by alternative splicing maintains the female determined state in *Drosophila*. *Cell* **65,** 229–239
7. Inoue, K., Hoshijima, K., Sakamoto, H., and Shimura, Y. (1990) Binding of the *Drosophila* sex-lethal gene product to the alternative splice site of transformer primary transcript. *Nature* **344,** 461–463
8. Kelley, R. L., Wang, J., Bell, L., and Kuroda, M. I. (1997) Sex lethal controls dosage compensation in *Drosophila* by a non-splicing mechanism. *Nature* **387,** 195–199
9. Flickinger, T. W., and Salz, H. K. (1994) The *Drosophila* sex determination gene *snf* encodes a nuclear protein with sequence and functional similarity to the mammalian U1A snRNP protein. *Genes Dev.* **8,** 914–925
10. Hilfiker, A., Amrein, H., Dübendorfer, A., Schneiter, R., and Nöthiger, R. (1995) The gene virilizer is required for female-specific splicing controlled by Sxl, the master gene for sexual development in *Drosophila*. *Development* **121,** 4017–4026
11. Granadino, B., Campuzano, S., and Sánchez, L. (1990) The *Drosophila melanogaster* fl(2)d gene is needed for the female-specific splicing of Sex-lethal RNA. *EMBO J.* **9,** 2597–2602
12. Ortega, A., Niksic, M., Bachi, A., Wilm, M., Sánchez, L., Hastie, N., and Valcárcel, J. (2003) Biochemical function of female-lethal (2)D/Wilms' tumor suppressor-1-associated proteins in alternative pre-mRNA splicing. *J. Biol. Chem.* **278,** 3040–3047
13. Penn, J. K., Graham, P., Deshpande, G., Calhoun, G., Chaouki, A. S., Salz, H. K., and Schedl, P. (2008) Functioning of the *Drosophila* Wilms'-tumor-1-associated protein homolog, Fl(2)d, in Sex-lethal-dependent alternative splicing. *Genetics* **178,** 737–748
14. Little, N. A., Hastie, N. D., and Davies, R. C. (2000) Identification of WTAP, a novel Wilms' tumour 1-associating protein. *Hum. Mol. Genet.* **9,** 2231–2239
15. Zhou, Z., Licklider, L. J., Gygi, S. P., and Reed, R. (2002) Comprehensive proteomic analysis of the human spliceosome. *Nature* **419,** 182–185
16. Saitoh, N., Spahr, C. S., Patterson, S. D., Bubulya, P., Neuwald, A. F., and Spector, D. L. (2004) Proteomic analysis of interchromatin granule clusters. *Mol. Biol. Cell* **15,** 3876–3890
17. Horiuchi, K., Umetani, M., Minami, T., Okayama, H., Takada, S., Yamamoto, M., Aburatani, H., Reid, P. C., Housman, D. E., Hamakubo, T., and Kodama, T. (2006) Wilms' tumor 1-associating protein regulates G2/M transition through stabilization of cyclin A2 mRNA. *Proc. Natl. Acad. Sci. U.S.A.* **103,** 17278–17283
18. Fukusumi, Y., Naruse, C., and Asano, M. (2008) Wtap is required for differentiation of endoderm and mesoderm in the mouse embryo. *Dev. Dyn.* **237,** 618–629
19. Small, T. W., Bolender, Z., Bueno, C., O'Neil, C., Nong, Z., Rushlow, W., Rajakumar, N., Kandel, C., Strong, J., Madrenas, J., and Pickering, J. G. (2006) Wilms' tumor 1-associating protein regulates the proliferation of vascular smooth muscle cells. *Circ. Res.* **99,** 1338–1346
20. Small, T. W., and Pickering, J. G. (2009) Nuclear degradation of Wilms tumor 1-associating protein and survivin splice variant switching underlie IGF-1-mediated survival. *J. Biol. Chem.* **284,** 24684–24695
21. Jin, D. I., Lee, S. W., Han, M. E., Kim, H. J., Seo, S. A., Hur, G. Y., Jung, S., Kim, B. S., and Oh, S. O. (2012) Expression and roles of Wilms' tumor 1-associating protein in glioblastoma. *Cancer Sci.* **103,** 2102–2109
22. Jo, H. J., Shim, H. E., Han, M. E., Kim, H. J., Kim, K. S., Baek, S., Choi, K. U., Hur, G. Y., and Oh, S. O. (January 25, 2013) WTAP regulates migration and invasion of cholangiocarcinoma cells. *J. Gastroenterol.* 10.1007/s00535-013-0748-7
23. Tanaka, T., Jiang, S., Hotta, H., Takano, K., Iwanari, H., Sumi, K., Daigo, K., Ohashi, R., Sugai, M., Ikegame, C., Umezu, H., Hirayama, Y., Midorikawa, Y., Hippo, Y., Watanabe, A., Uchiyama, Y., Hasegawa, G., Reid, P., Aburatani, H., Hamakubo, T., Sakai, J., Naito, M., and Kodama, T. (2006) Dysregulated expression of P1 and P2 promoter-driven hepatocyte nuclear factor-4α in the pathogenesis of human cancer. *J. Pathol.* **208,** 662–672
24. Daigo, K., Kawamura, T., Ohta, Y., Ohashi, R., Katayose, S., Tanaka, T., Aburatani, H., Naito, M., Kodama, T., Ihara, S., and Hamakubo, T. (2011) Proteomic analysis of native hepatocyte nuclear factor-4α (HNF4α) isoforms, phosphorylation status, and interactive cofactors. *J. Biol. Chem.* **286,** 674–686
25. Daigo, K., Yamaguchi, N., Kawamura, T., Matsubara, K., Jiang, S., Ohashi, R., Sudou, Y., Kodama, T., Naito, M., Inoue, K., and Hamakubo, T. (2012) The proteomic profile of circulating pentraxin 3 (PTX3) complex in sepsis demonstrates the interaction with azurocidin 1 and other components of neutrophil extracellular traps. *Mol. Cell. Proteomics* 10.1074/mcp.M111.015073
26. Tripathi, V., Ellis, J. D., Shen, Z., Song, D. Y., Pan, Q., Watt, A. T., Freier, S. M., Bennett, C. F., Sharma, A., Bubulya, P. A., Blencowe, B. J., Prasanth, S. G., and Prasanth, K. V. (2010) The nuclear-retained noncoding RNA MALAT1 regulates alternative splicing by modulating SR splicing factor phosphorylation. *Mol. Cell* **39,** 925–938
27. Fujita, Y., Krause, G., Scheffner, M., Zechner, D., Leddy, H. E., Behrens, J., Sommer, T., and Birchmeier, W. (2002) Hakai, a c-Cbl-like protein, ubiquitinates and induces endocytosis of the E-cadherin complex. *Nat. Cell Biol.* **4,** 222–231
28. Kaido, M., Wada, H., Shindo, M., and Hayashi, S. (2009) Essential requirement for RING finger E3 ubiquitin ligase Hakai in early embryonic development of Drosophila. *Genes Cells* **14,** 1067–1077
29. Figueroa, A., Kotani, H., Toda, Y., Mazan-Mamczarz, K., Mueller, E. C., Otto, A., Disch, L., Norman, M., Ramdasi, R. M., Keshtgar, M., Gorospe, M., and Fujita, Y. (2009) Novel roles of hakai in cell proliferation and oncogenesis. *Mol. Biol. Cell* **20,** 3533–3542
30. Mukherjee, M., Chow, S. Y., Yusoff, P., Seetharaman, J., Ng, C., Sinniah, S., Koh, X. W., Asgar, N. F., Li, D., Yim, D., Jackson, R. A., Yew, J., Qian, J., Iyu, A., Lim, Y. P., Zhou, X., Sze, S. K., Guy, G. R., and Sivaraman, J. (2012) Structure of a novel phosphotyrosine-binding domain in Hakai that targets E-cadherin. *EMBO J.* **31,** 1308–1319
31. Vasilescu, J., Guo, X., and Kast, J. (2004) Identification of protein-protein interactions using *in vivo* cross-linking and mass spectrometry. *Proteomics* **4,** 3845–3854
32. Kim, K. M., Yi, E. C., and Kim, Y. (2012) Mapping protein receptor-ligand interactions via *in vivo* chemical crosslinking, affinity purification, and differential mass spectrometry. *Methods* **56,** 161–165
33. Merz, C., Urlaub, H., Will, C. L., and Lührmann, R. (2007) Protein composition of human mRNPs spliced in vitro and differential requirements for mRNP protein recruitment. *RNA* **13,** 116–128
34. Lamond, A. I., and Spector, D. L. (2003) Nuclear speckles. A model for nuclear organelles. *Nat. Rev. Mol. Cell Biol.* **4,** 605–612
35. Clemson, C. M., Hutchinson, J. N., Sara, S. A., Ensminger, A. W., Fox, A. H., Chess, A., and Lawrence, J. B. (2009) An architectural role for a nuclear noncoding RNA. NEAT1 RNA is essential for the structure of paraspeckles. *Mol. Cell* **33,** 717–726
36. Hutchinson, J. N., Ensminger, A. W., Clemson, C. M., Lynch, C. R., Lawrence, J. B., and Chess, A. (2007) A screen for nuclear transcripts identifies two linked noncoding RNAs associated with SC35 splicing domains. *BMC Genomics* **8,** 39
37. Bernard, D., Prasanth, K. V., Tripathi, V., Colasse, S., Nakamura, T., Xuan, Z., Zhang, M. Q., Sedel, F., Jourdren, L., Coulpier, F., Triller, A., Spector, D. L., and Bessis, A. (2010) A long nuclear-retained non-coding RNA regulates synaptogenesis by modulating gene expression. *EMBO J.* **29,** 3082–3093
38. Tripathi, V., Shen, Z., Chakraborty, A., Giri, S., Freier, S. M., Wu, X., Zhang, Y., Gorospe, M., Prasanth, S. G., Lal, A., and Prasanth, K. V. (2013) Long noncoding RNA MALAT1 controls cell cycle progression by regu-

lating the expression of oncogenic transcription factor B-MYB. *PLoS Genet.* **9,** e1003368
39. Cook, D., Nuro, E., and Murai, K. K. (May 31, 2013) Increasing our understanding of human cognition through the study of fragile X syndrome. *Dev. Neurobiol.* 10.1002/dneu.22096
40. Amente, S., Napolitano, G., Licciardo, P., Monti, M., Pucci, P., Lania, L., and Majello, B. (2005) Identification of proteins interacting with the RNA-PII FCP1 phosphatase. FCP1 forms a complex with arginine methyltransferase PRMT5 and it is a substrate for PRMT5-mediated methylation. *FEBS Lett.* **579,** 683–689
41. Lukasik, A., Uniewicz, K. A., Kulis, M., and Kozlowski, P. (2008) Ciz1, a p21 cip1/Waf1-interacting zinc finger protein and DNA replication factor, is a novel molecular partner for human enhancer of rudimentary homolog. *FEBS J.* **275,** 332–340
42. Onyango, P., and Feinberg, A. P. (2011) A nucleolar protein, H19 opposite tumor suppressor (HOTS), is a tumor growth inhibitor encoded by a human imprinted H19 antisense transcript. *Proc. Natl. Acad. Sci. U.S.A.* **108,** 16759–16764
43. Smyk, A., Szuminska, M., Uniewicz, K. A., Graves, L. M., and Kozlowski, P. (2006) Human enhancer of rudimentary is a molecular partner of PDIP46/SKAR, a protein interacting with DNA polymerase δ and S6K1 and regulating cell growth. *FEBS J.* **273,** 4728–4741
44. Zafrakas, M., Losen, I., Knüchel, R., and Dahl, E. (2008) Enhancer of the rudimentary gene homologue (ERH) expression pattern in sporadic human breast cancer and normal breast tissue. *BMC Cancer* **8,** 145
45. Weng, M. T., Lee, J. H., Wei, S. C., Li, Q., Shahamatdar, S., Hsu, D., Schetter, A. J., Swatkoski, S., Mannan, P., Garfield, S., Gucek, M., Kim, M. K., Annunziata, C. M., Creighton, C. J., Emanuele, M. J., Harris, C. C., Sheu, J. C., Giaccone, G., and Luo, J. (2012) Evolutionarily conserved protein ERH controls CENP-E mRNA splicing and is required for the survival of KRAS mutant cancer cells. *Proc. Natl. Acad. Sci. U.S.A.* **109,** E3659–E3667
46. Fujimura, A., Kishimoto, H., Yanagisawa, J., and Kimura, K. (2012) Enhancer of rudimentary homolog (ERH) plays an essential role in the progression of mitosis by promoting mitotic chromosome alignment. *Biochem. Biophys. Res. Commun.* **423,** 588–592
47. Zhong, S., Li, H., Bodi, Z., Button, J., Vespa, L., Herzog, M., and Fray, R. G. (2008) MTA is an *Arabidopsis* messenger RNA adenosine methylase and interacts with a homolog of a sex-specific splicing factor. *Plant Cell* **20,** 1278–1288
48. Potashkin, J., Kim, D., Fons, M., Humphrey, T., and Frendewey, D. (1998) Cell-division-cycle defects associated with fission yeast pre-mRNA splicing mutants. *Curr. Genet.* **34,** 153–163
49. Anczuków, O., Rosenberg, A. Z., Akerman, M., Das, S., Zhan, L., Karni, R., Muthuswamy, S. K., and Krainer, A. R. (2012) The splicing factor SRSF1 regulates apoptosis and proliferation to promote mammary epithelial cell transformation. *Nat. Struct. Mol. Biol.* **19,** 220–228
50. He, X., Arslan, A. D., Pool, M. D., Ho, T. T., Darcy, K. M., Coon, J. S., and Beck, W. T. (2011) Knockdown of splicing factor SRp20 causes apoptosis in ovarian cancer cells and its expression is associated with malignancy of epithelial ovarian cancer. *Oncogene* **30,** 356–365
51. Karni, R., de Stanchina, E., Lowe, S. W., Sinha, R., Mu, D., and Krainer, A. R. (2007) The gene encoding the splicing factor SF2/ASF is a proto-oncogene. *Nat. Struct. Mol. Biol.* **14,** 185–193
52. Schwerk, C., and Schulze-Osthoff, K. (2005) Regulation of apoptosis by alternative pre-mRNA splicing. *Mol. Cell* **19,** 1–13
53. Li, X., and Manley, J. L. (2005) Inactivation of the SR protein splicing factor ASF/SF2 results in genomic instability. *Cell* **122,** 365–378
54. Li, X., Wang, J., and Manley, J. L. (2005) Loss of splicing factor ASF/SF2 induces G2 cell cycle arrest and apoptosis, but inhibits internucleosomal DNA fragmentation. *Genes Dev.* **19,** 2705–2714
55. Xiao, R., Sun, Y., Ding, J. H., Lin, S., Rose, D. W., Rosenfeld, M. G., Fu, X. D., and Li, X. (2007) Splicing regulator SC35 is essential for genomic stability and cell proliferation during mammalian organogenesis. *Mol. Cell. Biol.* **27,** 5393–5402
56. Horabin, J. I., and Schedl, P. (1993) Sex-lethal autoregulation requires multiple cis-acting elements upstream and downstream of the male exon and appears to depend largely on controlling the use of the male exon 5′ splice site. *Mol. Cell. Biol.* **13,** 7734–7746
57. Sakamoto, H., Inoue, K., Higuchi, I., Ono, Y., and Shimura, Y. (1992) Control of *Drosophila* Sex-lethal pre-mRNA splicing by its own female-specific product. *Nucleic Acids Res.* **20,** 5533–5540
58. Wang, J., and Bell, L. R. (1994) The Sex-lethal amino terminus mediates cooperative interactions in RNA binding and is essential for splicing regulation. *Genes Dev.* **8,** 2072–2085
59. Sosnowski, B. A., Belote, J. M., and McKeown, M. (1989) Sex-specific alternative splicing of RNA from the transformer gene results from sequence-dependent splice site blockage. *Cell* **58,** 449–459
60. Valcárcel, J., Singh, R., Zamore, P. D., and Green, M. R. (1993) The protein Sex-lethal antagonizes the splicing factor U2AF to regulate alternative splicing of transformer pre-mRNA. *Nature* **362,** 171–175
61. Förch, P., Merendino, L., Martínez, C., and Valcárcel, J. (2001) Modulation of msl-2 5′ splice site recognition by Sex-lethal. *RNA* **7,** 1185–1191
62. Merendino, L., Guth, S., Bilbao, D., Martínez, C., and Valcárcel, J. (1999) Inhibition of msl-2 splicing by Sex-lethal reveals interaction between U2AF35 and the 3′ splice site AG. *Nature* **402,** 838–841